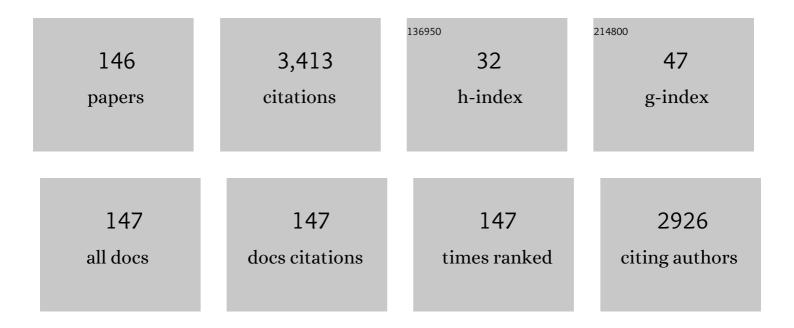
## List of Publications by Year in descending order

Source: https://exaly.com/author-pdf/1035048/publications.pdf Version: 2024-02-01



XIIWANG

#	Article	lF	CITATIONS
1	High-Yield Production of Highly Fluorinated Graphene by Direct Heating Fluorination of Graphene-oxide. ACS Applied Materials & amp; Interfaces, 2013, 5, 8294-8299.	8.0	152
2	Molecular packing and properties of poly(benzoxazole-benzimidazole-imide) copolymers. Polymer Chemistry, 2012, 3, 1517.	3.9	106
3	The evolution of macromolecular packing and sudden crystallization in rigid-rod polyimide via effect of multiple H-bonding on charge transfer (CT) interactions. Polymer, 2014, 55, 4258-4269.	3.8	92
4	Recent Advances in Fluorinated Graphene from Synthesis to Applications: Critical Review on Functional Chemistry and Structure Engineering. Advanced Materials, 2022, 34, e2101665.	21.0	90
5	Fluorographene with High Fluorine/Carbon Ratio: A Nanofiller for Preparing Low-κ Polyimide Hybrid Films. ACS Applied Materials & Interfaces, 2014, 6, 16182-16188.	8.0	85
6	Toward Excellent Tribological Performance as Oil-Based Lubricant Additive: Particular Tribological Behavior of Fluorinated Graphene. ACS Applied Materials & Interfaces, 2018, 10, 28828-28838.	8.0	85
7	Correlation between hydrogenâ€bonding interaction and mechanical properties of polyimide fibers. Polymers for Advanced Technologies, 2009, 20, 362-366.	3.2	75
8	Mechanically Strong Chitin Fibers with Nanofibril Structure, Biocompatibility, and Biodegradability. Chemistry of Materials, 2019, 31, 2078-2087.	6.7	66
9	Characterization of Conformation and Locations of C–F Bonds in Graphene Derivative by Polarized ATR-FTIR. Analytical Chemistry, 2016, 88, 3926-3934.	6.5	63
10	Surface modification of strontium-doped porous bioactive ceramic scaffolds via poly(DOPA) coating and immobilizing silk fibroin for excellent angiogenic and osteogenic properties. Biomaterials Science, 2016, 4, 678-688.	5.4	56
11	Mechanically Strong Multifilament Fibers Spun from Cellulose Solution via Inducing Formation of Nanofibers. ACS Sustainable Chemistry and Engineering, 2018, 6, 5314-5321.	6.7	56
12	Towards enhanced tribological performance as water-based lubricant additive: Selective fluorination of graphene oxide at mild temperature. Journal of Colloid and Interface Science, 2018, 531, 138-147.	9.4	56
13	Ω-Shaped Fiber-Optic Probe-Based Localized Surface Plasmon Resonance Biosensor for Real-Time Detection of <i>Salmonella</i> Typhimurium. Analytical Chemistry, 2018, 90, 13640-13646.	6.5	55
14	Controllable defluorination of fluorinated graphene and weakening of C–F bonding under the action of nucleophilic dipolar solvent. Physical Chemistry Chemical Physics, 2016, 18, 3285-3293.	2.8	54
15	Ester Crosslinking Enhanced Hydrophilic Cellulose Nanofibrils Aerogel. ACS Sustainable Chemistry and Engineering, 2018, 6, 11979-11988.	6.7	51
16	Surface modification of PBO fibers by direct fluorination and corresponding chemical reaction mechanism. Composites Science and Technology, 2018, 165, 106-114.	7.8	49
17	In-situ polymerization and covalent modification on aramid fiber surface via direct fluorination for interfacial enhancement. Composites Part B: Engineering, 2020, 182, 107608.	12.0	48
18	Effects of the oxygenic groups on the mechanism of fluorination of graphene oxide and its structure. Physical Chemistry Chemical Physics, 2017, 19, 5504-5512.	2.8	47

#	Article	IF	CITATIONS
19	Influences of Coagulation Conditions on the Structure and Properties of Regenerated Cellulose Filaments via Wet-Spinning in LiOH/Urea Solvent. ACS Sustainable Chemistry and Engineering, 2018, 6, 4056-4067.	6.7	47
20	Structure and properties of novel PMDA/ODA/PABZ polyimide fibers. Polymer Engineering and Science, 2008, 48, 912-917.	3.1	44
21	Nondestructive grafting of PEI on aramid fiber surface through the coordination of Fe (â¢) to enhance composite interfacial properties. Applied Surface Science, 2017, 401, 323-332.	6.1	43
22	Aligned fluorinated single-walled carbon nanotubes as a transmission channel towards attenuation of broadband electromagnetic waves. Journal of Materials Chemistry C, 2018, 6, 9399-9409.	5.5	43
23	Chemical reactivity of C–F bonds attached to graphene with diamines depending on their nature and location. Physical Chemistry Chemical Physics, 2016, 18, 17495-17505.	2.8	42
24	Graphene-based porous materials with tunable surface area and CO2 adsorption properties synthesized by fluorine displacement reaction with various diamines. Journal of Colloid and Interface Science, 2016, 478, 36-45.	9.4	42
25	Highly improved Uv resistance and composite interfacial properties of aramid fiber via iron (III) coordination. Applied Surface Science, 2018, 434, 473-480.	6.1	42
26	The introduction of asymmetric heterocyclic units into poly(p-phenylene terephthalamide) and its effect on microstructure, interactions and properties. Journal of Materials Science, 2018, 53, 13291-13303.	3.7	41
27	Covalent functionalization of fluorinated graphene through activation of dormant radicals for water-based lubricants. Carbon, 2020, 167, 826-834.	10.3	41
28	Reduction and transformation of fluorinated graphene induced by ultraviolet irradiation. Physical Chemistry Chemical Physics, 2015, 17, 24056-24062.	2.8	39
29	Characterization of the thermal/thermal oxidative stability of fluorinated graphene with various structures. Physical Chemistry Chemical Physics, 2017, 19, 19442-19451.	2.8	37
30	Excellent Microwave Absorbing Property of Multiwalled Carbon Nanotubes with Skin–Core Heterostructure Formed by Outer Dominated Fluorination. Journal of Physical Chemistry C, 2018, 122, 6357-6367.	3.1	37
31	Activation effect of porous structure on fluorination of graphene based materials with large specific surface area at mild condition. Carbon, 2017, 124, 288-295.	10.3	35
32	Flexible pressure sensors with high pressure sensitivity and low detection limit using a unique honeycomb-designed polyimide/reduced graphene oxide composite aerogel. RSC Advances, 2021, 11, 11760-11770.	3.6	35
33	The wear-resistance of composite depending on the interfacial interaction between thermoplastic polyurethane and fluorinated UHMWPE particles with or without oxygen. Composites Science and Technology, 2015, 106, 68-75.	7.8	34
34	Dependence of the fluorination intercalation of graphene toward high-quality fluorinated graphene formation. Chemical Science, 2019, 10, 5546-5555.	7.4	33
35	Preparation and characterization of novel polyimide films containing amide groups. Journal of Polymer Research, 2012, 19, 1.	2.4	31
36	Control of Head/Tail Isomeric Structure in Polyimide and Isomerismâ€Derived Difference in Molecular Packing and Properties. Macromolecular Rapid Communications, 2017, 38, 1700404.	3.9	30

#	Article	IF	CITATIONS
37	The novel high performance aramid fibers containing benzimidazole moieties and chloride substitutions. Materials and Design, 2018, 158, 127-135.	7.0	30
38	Feasibility study of the naturally occurring dialdehyde carboxymethyl cellulose for biological tissue fixation. Carbohydrate Polymers, 2015, 115, 54-61.	10.2	29
39	Effect of molecular rigidity and hydrogen bond interaction on mechanical properties of polyimide fibers. Journal of Applied Polymer Science, 2016, 133, .	2.6	29
40	Crosslinking effect of dialdehyde starch (DAS) on decellularized porcine aortas for tissue engineering. International Journal of Biological Macromolecules, 2015, 79, 813-821.	7.5	28
41	Defluorination and covalent grafting of fluorinated graphene with TEMPO in a radical mechanism. Physical Chemistry Chemical Physics, 2017, 19, 24076-24081.	2.8	28
42	Constructing mainstay-body structure in heterocyclic aramid fiber to simultaneously improve tensile strength and toughness. Composites Part B: Engineering, 2020, 202, 108411.	12.0	28
43	Cove-Edged Graphene Nanoribbons with Incorporation of Periodic Zigzag-Edge Segments. Journal of the American Chemical Society, 2022, 144, 228-235.	13.7	28
44	Enhancement of properties of polyimide/silica hybrid nanocomposites by benzimidazole formed hydrogen bond. Polymers for Advanced Technologies, 2012, 23, 1362-1368.	3.2	27
45	Facile preparation of highly hydrophilic, recyclable high-performance polyimide adsorbents for the removal of heavy metal ions. Journal of Hazardous Materials, 2016, 306, 210-219.	12.4	26
46	Towards efficient microwave absorption: intrinsic heterostructure of fluorinated SWCNTs. Journal of Materials Chemistry C, 2017, 5, 11847-11855.	5.5	26
47	The particular phase transformation during graphene fluorination process. Carbon, 2018, 132, 271-279.	10.3	26
48	A facile strategy for fabricating aramid fiber with simultaneously high compressive strength and high interfacial shear strength through cross-linking promoted by oxygen. Composites Part A: Applied Science and Manufacturing, 2018, 113, 233-241.	7.6	26
49	Skin–core structured fluorinated MWCNTs: a nanofiller towards a broadband dielectric material with a high dielectric constant and low dielectric loss. Journal of Materials Chemistry C, 2018, 6, 2370-2378.	5.5	25
50	The dominant factor for mechanical property of polyimide films containing heterocyclic moieties: Inâ€plane orientation, crystallization, or hydrogen bonding. Journal of Applied Polymer Science, 2016, 133, .	2.6	24
51	A facile method to enhance UV stability of PBIA fibers with intense fluorescence emission by forming complex with hydrogen chloride on the fibers surface. Polymer Degradation and Stability, 2016, 128, 278-285.	5.8	24
52	Pre-drawing induced evolution of phase, microstructure and property in para-aramid fibres containing benzimidazole moiety. RSC Advances, 2016, 6, 62695-62704.	3.6	24
53	Novel aromatic polyimide fiber with biphenyl side-groups: Dope synthesis and filament internal morphology control. Polymer Engineering and Science, 2006, 46, 123-128.	3.1	23
54	One-Step Preparation of Oxygen/Fluorine Dual Functional MWCNTs with Good Water Dispersibility by the Initiation of Fluorine Gas. ACS Applied Materials & Interfaces, 2016, 8, 7991-7999.	8.0	23

#	Article	IF	CITATIONS
55	Antibacterial activities and mechanisms of fluorinated graphene and guanidine-modified graphene. RSC Advances, 2016, 6, 8763-8772.	3.6	23
56	Radical chain reaction mechanism of graphene fluorination. Carbon, 2018, 137, 451-457.	10.3	22
57	The Friedel–Crafts reaction of fluorinated graphene for high-yield arylation of graphene. Chemical Communications, 2018, 54, 10168-10171.	4.1	22
58	Constructing a weaving structure for aramid fiber by carbon nanotube-based network to simultaneously improve composites interfacial properties and compressive properties. Composites Science and Technology, 2019, 182, 107721.	7.8	22
59	Fabrication of durable hierarchical superhydrophobic fabrics with Sichuan pepper-like structures via graft precipitation polymerization. Applied Surface Science, 2020, 529, 147017.	6.1	22
60	Biocompatibility and anti-calcification of a biological artery immobilized with naturally-occurring phytic acid as the crosslinking agent. Journal of Materials Chemistry B, 2017, 5, 8115-8124.	5.8	21
61	Enhanced Osteoconductivity and Osseointegration in Calcium Polyphosphate Bioceramic Scaffold via Lithium Doping for Bone Regeneration. ACS Biomaterials Science and Engineering, 2019, 5, 5872-5880.	5.2	21
62	Bioinspired three-dimensional and multiple adsorption effects toward high lubricity of solvent-free graphene-based nanofluid. Carbon, 2022, 188, 166-176.	10.3	21
63	Construction of dendritic structure by nano-SiO2 derivate grafted with hyperbranched polyamide in aramid fiber to simultaneously improve its mechanical and compressive properties. European Polymer Journal, 2019, 119, 367-375.	5.4	20
64	Green and Economical Strategy for Spinning Robust Cellulose Filaments. ACS Sustainable Chemistry and Engineering, 2020, 8, 14927-14937.	6.7	20
65	The Effect of Asymmetric Heterocyclic Units on the Microstructure and the Improvement of Mechanical Properties of Three Rigidâ€Rod coâ€PI Fibers. Macromolecular Materials and Engineering, 2016, 301, 853-863.	3.6	19
66	Radical mechanism of a nucleophilic reaction depending on a two-dimensional structure. Physical Chemistry Chemical Physics, 2018, 20, 489-497.	2.8	19
67	Nondestructive modification of aramid fiber based on selective reaction of external cross-linker to improve interfacial shear strength and compressive strength. Composites Part A: Applied Science and Manufacturing, 2019, 119, 217-224.	7.6	19
68	Bioinspired, Artificial, Small-Diameter Vascular Grafts with Selective and Rapid Endothelialization Based on an Amniotic Membrane-Derived Hydrogel. ACS Biomaterials Science and Engineering, 2020, 6, 1603-1613.	5.2	19
69	Spontaneous power generation from broad-humidity atmospheres through heterostructured F/O-bonded graphene monoliths. Nano Energy, 2022, 91, 106605.	16.0	19
70	Preparation of Thermosetting/Thermoplastic Polyimide Foam with Pleated Cellular Structure via In Situ Simultaneous Orthogonal Polymerization. ACS Applied Polymer Materials, 2019, 1, 2430-2440.	4.4	18
71	Investigation of the dispersion behavior of fluorinated MWCNTs in various solvents. Physical Chemistry Chemical Physics, 2017, 19, 21565-21574.	2.8	17
72	Toward high-efficiency photoluminescence emission by fluorination of graphene oxide: Investigations from excitation to emission evolution. Carbon, 2020, 165, 386-394.	10.3	17

#	Article	IF	CITATIONS
73	Low temperature preparation of highly fluorinated multiwalled carbon nanotubes activated by Fe <sub>3</sub> O <sub>4</sub> to enhance microwave absorbing property. Nanotechnology, 2018, 29, 365703.	2.6	16
74	Noticeably enhanced microwave absorption performance via constructing molecular-level interpenetrating carbon network heterostructure. Carbon, 2021, 183, 858-871.	10.3	16
75	Controllable construction of Fluorine-Contained phase region induced by fluorination phase Transformation: Towards enhanced microwave absorption of carbon foam. Chemical Engineering Journal, 2022, 446, 137408.	12.7	16
76	Dependence of pretilt angle on orientation and conformation of side chain with different chemical structure in polyimide film surface. RSC Advances, 2012, 2, 9463.	3.6	15
77	Highâ€performance copoly(benzimidazoleâ€benzoxazoleâ€imide) fibers: Fabrication, structure, and properties. Journal of Applied Polymer Science, 2015, 132, .	2.6	15
78	Synthesis of Heterocyclic Aramid Fiber Based on Solidâ€Phase Crossâ€Linking of Oligomers with Reactive End Group. Macromolecular Materials and Engineering, 2018, 303, 1800076.	3.6	15
79	Giant Enhancement of Fluorescence Emission by Fluorination of Porous Graphene with High Defect Density and Subsequent Application as Fe <sup>3+</sup> Ion Sensors. ACS Applied Materials & Interfaces, 2020, 12, 40662-40672.	8.0	15
80	Regulating Cu(II)-benzimidazole coordination structure in rigid-rod aramid fiber and its composites enhancement effects. Composites Science and Technology, 2019, 184, 107837.	7.8	14
81	In Situ Radical Polymerization and Grafting Reaction Simultaneously Initiated by Fluorinated Graphene. Langmuir, 2019, 35, 6610-6619.	3.5	14
82	Regulating the Bonding Nature and Location of C–F Bonds in Fluorinated Graphene by Doping Nitrogen Atoms. Industrial & Engineering Chemistry Research, 2021, 60, 875-884.	3.7	14
83	Post-construction of weaving structure in aramid fiber towards improvements of its transverse properties. Composites Science and Technology, 2021, 208, 108780.	7.8	14
84	Enhancing mechanical properties of aromatic polyamide fibers containing benzimidazole units via temporarily suppressing hydrogen bonding and crystallization. Journal of Applied Polymer Science, 2015, 132, .	2.6	13
85	The evolution of structure and properties for copolyamide fibers–containing benzimidazole units during the decomplexation of hydrogen chloride. High Performance Polymers, 2016, 28, 381-389.	1.8	13
86	Defluorination-assisted heteroatom doping reaction with ammonia gas for synthesis of nitrogen-doped porous graphitized carbon. Chemical Engineering Journal, 2018, 354, 261-268.	12.7	13
87	Preparation of novel aramid film with ultra-high breakdown strength via constructing three-dimensional covalent crosslinked structure. Chemical Engineering Journal, 2019, 375, 122042.	12.7	13
88	Thermal stability of C–F/C(–F) <sub>2</sub> bonds in fluorinated graphene detected by <i>in situ</i> heating infrared spectroscopy. Physical Chemistry Chemical Physics, 2021, 23, 26853-26863.	2.8	13
89	The reaction kinetics and mechanism of crude fluoroelastomer vulcanized by direct fluorination with fluorine/nitrogen gas. RSC Advances, 2015, 5, 18932-18938.	3.6	12
90	Various surface functionalizations of ultra-high-molecular-weight polyethylene based on fluorine-activation behavior. RSC Advances, 2015, 5, 79081-79089.	3.6	12

#	Article	IF	CITATIONS
91	Benzimidazole-containing aramid nanofiber for naked-eye detection of heavy metal ions. Analyst, The, 2018, 143, 5225-5233.	3.5	12
92	A promising material for bone repair: PMMA bone cement modified by dopamine-coated strontium-doped calcium polyphosphate particles. Royal Society Open Science, 2019, 6, 191028.	2.4	12
93	Preparation of High Strength and Toughness Aramid Fiber by Introducing Flexible Asymmetric Monomer to Construct Misplacedâ€Nunchaku Structure. Macromolecular Materials and Engineering, 2021, 306, 2000814.	3.6	12
94	Catalysis and inhibition of benzimidazole units on thermal imidization of poly(amic acid) via hydrogen bonding interactions. Chinese Journal of Polymer Science (English Edition), 2015, 33, 621-632.	3.8	11
95	Radical Mechanism for the Reduction of Graphene Derivatives Initiated by Electron-Transfer Reactions. Journal of Physical Chemistry C, 2018, 122, 8473-8479.	3.1	11
96	Fluorination-generated uninterrupted gradient-refractive index on commercial flexible substrates for high broadband and omnidirectional transmittance. Applied Surface Science, 2019, 489, 494-503.	6.1	11
97	Preparing Nitrogen-Doped Multiwalled Carbon Nanotubes with Regionally Controllable Heterojunction Structure by Nondestructive Postdoping with the Assistance of Heating Fluorination. Journal of Physical Chemistry C, 2019, 123, 16439-16448.	3.1	10
98	Direct fluorination as a one-step ATRP initiator immobilization for convenient surface grafting of phenyl ring-containing substrates. Polymer Chemistry, 2020, 11, 5693-5700.	3.9	10
99	Fabrication of Grapheneâ€Based Selfâ€Assembly Monoliths through Reversible Fluorination and Defluorination Strategy. Advanced Materials Interfaces, 2020, 7, 2000915.	3.7	10
100	A novel CPC composite cement reinforced by dopamine coated SCPP fibers with improved physicochemical and biological properties. Materials Science and Engineering C, 2020, 109, 110544.	7.3	10
101	Effect of a biphenyl side chain of polyimide on the pretilt angle of liquid crystal molecules: molecular simulation and experimental studies. Liquid Crystals, 2010, 37, 149-158.	2.2	9
102	In situ preparation and characterization of polyimide/silica composite hemispheres by inverse aqueous emulsion technique and sol-gel method. Colloid and Polymer Science, 2015, 293, 1281-1287.	2.1	9
103	Thermally Robust Bendable Silicon Dioxide/Polyimide Layered Composite Film Through Catalytic Fluorination. ACS Applied Polymer Materials, 2019, 1, 777-786.	4.4	9
104	Nitrogen-Doping Chemical Behavior of Graphene Materials with Assistance of Defluorination. Journal of Physical Chemistry C, 2019, 123, 584-592.	3.1	9
105	Deliquification of Low-Productivity Natural Gas Wells with In Situ Generated Foams and Heat. Energy & Fuels, 2021, 35, 9873-9882.	5.1	9
106	Preparation of vertical alignment layers by blending polyimide precursors with and without side chains. Liquid Crystals, 2009, 36, 173-178.	2.2	8
107	Study of the orientation of liquid crystal molecules on polyimide alignment films by FTIR with polarisation mode. Liquid Crystals, 2012, 39, 813-817.	2.2	8
108	A composite with excellent tribological performance derived from oxy-fluorinated UHMWPE particle/polyurethane. RSC Advances, 2014, 4, 9321.	3.6	8

#	Article	IF	CITATIONS
109	Combination of support vector regression (SVR) and microwave plasma atomic emission spectrometry (MWP-AES) for quantitative elemental analysis in solid samples using the continuous direct solid sampling (CDSS) technique. Journal of Analytical Atomic Spectrometry, 2018, 33, 1954-1961.	3.0	8
110	Design and Electrical Analysis of Multi-Electrode Cylindrical Dielectric Barrier Discharge Plasma Reactor. IEEE Transactions on Plasma Science, 2019, 47, 419-426.	1.3	8
111	Suzuki–Miyaura reaction of C–F bonds in fluorographene. Chemical Communications, 2021, 57, 351-354.	4.1	8
112	Theoretical Calculations and Experiments on the Thermal Properties of Fluorinated Graphene and Its Effects on the Thermal Decomposition of Nitrate Esters. Nanomaterials, 2022, 12, 621.	4.1	8
113	Stretching induced steric interaction between backbone and side chain in a novel polyimide fiber. Polymer Engineering and Science, 2009, 49, 1225-1233.	3.1	7
114	Controlled drug release from a novel drug carrier of calcium polyphosphate/chitosan/aldehyde alginate scaffolds containing chitosan microspheres. RSC Advances, 2014, 4, 24810.	3.6	7
115	In vitro study of strontium doped calcium polyphosphate-modified arteries fixed by dialdehyde carboxymethyl cellulose for vascular scaffolds. International Journal of Biological Macromolecules, 2016, 93, 1583-1590.	7.5	7
116	Free Hâ€Bonding Interaction Sites in Rigid hain Polymers and Their Filling Approach: A Molecular Dynamics Simulation Study. Advanced Theory and Simulations, 2021, 4, 2100016.	2.8	7
117	Heating-activated radicals of fluorinated multiwalled carbon nanotubes assisted interfacial grafting rubber composites with electromagnetic wave absorption. Composites Science and Technology, 2021, 214, 108977.	7.8	7
118	The influence of fluorine atoms introduced into the surface of polyimide films by direct fluorination on the liquid crystal alignment. Liquid Crystals, 2009, 37, 115-119.	2.2	6
119	Ultrahigh strength and modulus copolyamide films with uniaxially cold-drawing induced molecular orientation. High Performance Polymers, 2017, 29, 58-67.	1.8	6
120	Introducing copper and collagen ( <i>via</i> poly(DOPA)) coating to activate inert ceramic scaffolds for excellent angiogenic and osteogenic capacity. RSC Advances, 2018, 8, 15575-15586.	3.6	6
121	In Situ Complex with byâ€product HCl and Release Chloride Ions to Dissolve Aramid. ChemPhysChem, 2018, 19, 2468-2471.	2.1	6
122	Increasing pretilt angle by grafting hexafluorobutyl acrylate into the surface of polyimide alignment films via electron beam irradiation. Liquid Crystals, 2013, 40, 435-440.	2.2	5
123	Influence of hydrogenâ€bonding interaction introduced by filled oligomer on bulk properties of blended polyimide films. Journal of Applied Polymer Science, 2014, 131, .	2.6	5
124	Improving Compressive Strength of Aramid Fiber by Introducing Carbon Nanotube Derivates Grafted with Oligomers of Different Conformations and Controlling Its Alignment. Macromolecular Materials and Engineering, 2019, 304, 1900127.	3.6	5
125	Improving Interfacial and Compressive Properties of Aramid by Synchronously Grafting and Crosslinking. Macromolecular Materials and Engineering, 2019, 304, 1900044.	3.6	5
126	Synthesis of tautomerization-inhibited diamino substituted tetraphenylethene derivatives with different mechanochromisms: the vital role of chlorine. Materials Chemistry Frontiers, 2021, 5, 2387-2398.	5.9	5

#	Article	IF	CITATIONS
127	Direct fluorination of nanographene molecules with fluorine gas. Carbon, 2022, 188, 453-460.	10.3	5
128	Homogeneous Fluorine Distribution in Graphene through Thermal Dissociation of Molecular F <sub>2</sub> : Implications for Thermal Conduction and Electrical Insulation. ACS Applied Nano Materials, 2022, 5, 6770-6780.	5.0	5
129	Correlation of pretilt angles and surface chemical structures of polyimide alignment films after direct fluorination. Polymer International, 2010, 59, 1622-1629.	3.1	4
130	Synergistic "Anchor―Effect of Carbon Nanotubes and Silica: A Facile and Efficient Double-Nanocomposite System To Reinforce High-Performance Polyimide Fibers. Industrial & Engineering Chemistry Research, 2019, 58, 16620-16628.	3.7	4
131	Dissolution of Aramid by Ionization of Byproduct HCl Promoted by Acetate. ChemistrySelect, 2019, 4, 123-129.	1.5	4
132	Câ^'N Coupling Reactions on Graphene with Aromatic Macromolecules and the Spatial Conformation of Grafted Macromolecules. Chemistry - A European Journal, 2020, 26, 1819-1826.	3.3	4
133	Reaction Performance and Flow Behavior of Isobutane/1-Butene and H <sub>2</sub> SO <sub>4</sub> in the Microreactor Configured with the Micro-mixer. Industrial & Engineering Chemistry Research, 2022, 61, 9122-9135.	3.7	4
134	Heterojunction of the CoMn Metal–Organic Framework with Lanthanum for Enhanced Oxygen Evolution Reaction. ACS Applied Energy Materials, 2022, 5, 8686-8696.	5.1	4
135	Crystallization of inorganic silica based on interaction between polyimide and silica by sol–gel method. Journal of Sol-Gel Science and Technology, 2013, 66, 193-198.	2.4	3
136	Synthesis of A Novel Crossâ€linker with High Reactivity for Enhancing Compressive Strength of Highâ€performance Organic Fibers. ChemistrySelect, 2019, 4, 3980-3983.	1.5	2
137	The adsorption of aromatic macromolecules on graphene with entropy-tailored behavior and its utilization in exfoliating graphite. Journal of Colloid and Interface Science, 2021, 599, 12-22.	9.4	2
138	Oxidative evolution of <i>Z</i> / <i>E</i> -diaminotetraphenylethylene. Physical Chemistry Chemical Physics, 2022, 24, 1960-1964.	2.8	2
139	Effect of surface modification of <scp>SiO<sub>2</sub></scp> particles on the interfacial and mechanical properties of <scp>PBS</scp> composites. Polymer Composites, 2022, 43, 5087-5094.	4.6	2
140	Effect of the skeleton structures in the side chain of polyimides on their film surface properties and pretilt angles of liquid crystal molecules. Liquid Crystals, 2010, 37, 1013-1019.	2.2	1
141	Preparation of novel polyimides containing aryl ester side chains end-capped with alkoxy groups and studies on their surface properties. Liquid Crystals, 2010, 37, 399-406.	2.2	1
142	Preparation and investigation of novel SrCl2/DCMC-modified (via DOPA) decellularized arteries with excellent physicochemical properties and cytocompatibility for vascular scaffolds. RSC Advances, 2018, 8, 30098-30105.	3.6	1
143	Shape and phase controlled synthesis of mesostructured carbon single crystals through mesoscale self-assembly of reactive monomicelles and their unprecedented exfoliation into single-layered carbon nanoribbons. Journal of Colloid and Interface Science, 2020, 558, 32-37.	9.4	1
144	Preparation and characterization of lithiumâ€8â€hydroxyquinolateâ€containing quaternary ammonium copolymers and their electrostatic layerâ€byâ€layer selfâ€assembly. Journal of Applied Polymer Science, 2008, 110, 124-133.	2.6	0

#	Article	IF	CITATIONS
145	The effect of Trimethylchlorosilane as a reactive additive on solution behavior of polyamide acid and properties of corresponding polyimide. Journal of Polymer Research, 2014, 21, 1.	2.4	Ο
146	Allâ€organic filler with fractal structure for reinforcement and toughening of aromatic polyamide film. Macromolecular Materials and Engineering, 0, , 2200031.	3.6	0